

The Primordial Black Hole Dark Matter - LISA Serendipity

N. Bartolo,^{1,2,3} V. De Luca,⁴ G. Franciolini,⁴ M. Peloso,^{1,2} and A. Riotto⁴

¹*Dipartimento di Fisica e Astronomia "G. Galilei",*

Università degli Studi di Padova, via Marzolo 8, I-35131 Padova, Italy

²*INFN, Sezione di Padova, via Marzolo 8, I-35131 Padova, Italy*

³*INAF - Osservatorio Astronomico di Padova, Vicolo dell'Osservatorio 5, I-35122 Padova, Italy*

⁴*Département de Physique Théorique and Centre for Astroparticle Physics (CAP),*

Université de Genève, 24 quai E. Ansermet, CH-1211 Geneva, Switzerland

(Dated: Thursday 1st September, 2022)

The last few years have witnessed a renewed interest in the possibility that primordial black holes (PBHs) constitute the dark matter of the universe. Current observational constraints leave only a few PBH mass ranges for this possibility. One of them is around $10^{-12}M_{\odot}$. If these PBHs are due to enhanced scalar perturbations produced during inflation, their formation is inevitably accompanied by the generation of fully non-Gaussian gravitational waves (GWs) with frequency peaked in the mHz range, precisely at the maximum sensitivity of the LISA mission. We show that, if these primordial black holes are the dark matter, LISA will be able to detect the GW power spectrum. However, despite the large primordial non-Gaussian three-point GW correlator, the propagation effects across the inhomogeneous universe decorrelate the phases of the GWs, largely suppressing the level of non-Gaussianity at detection. This general point, which has passed unnoticed in the recent literature, makes the scenario testable as LISA should measure only the two-point correlator.

Introduction. The existence and the nature of dark matter remains one of the main puzzles in physics [1]. The recent detection of GWs generated by the merging of two $\sim 30M_{\odot}$ black holes [2] has renewed the interest in the possibility that all (or a significant part of) the dark matter of the universe is in the form of PBHs (see Refs. [3–6] for recent literature).

A standard way to generate PBHs in the early universe is to enhance at small scales (small compared to the CMB ones) the power of the comoving curvature perturbation ζ during inflation [7–9] (see Ref. [10] in the case in which Standard Model Higgs perturbations are used). Such large perturbations are subsequently transferred to radiation through the reheating process after inflation, giving rise to PBHs upon horizon re-entry if they are large enough. A region collapses to a PBH if the density contrast (during the radiation era) $\Delta(\vec{x}) = (4/9a^2H^2)\nabla^2\zeta(\vec{x})$ is larger than a critical value Δ_c , which is a function of the shape of the power spectrum [11].

We define the comoving curvature perturbation power spectrum as

$$\langle\zeta(\vec{k}_1)\zeta(\vec{k}_2)\rangle' = \frac{2\pi^2}{k_1^3}\mathcal{P}_{\zeta}(k_1), \quad (1)$$

where we have adopted the standard prime notation indicating we do not explicitly write down the $(2\pi)^3$ times the Dirac delta of momentum conservation. It is convenient to define the variance of $\Delta(\vec{x})$ as

$$\sigma_{\Delta}^2(M) = \int_0^{\infty} d\ln k W^2(k, R_H)\mathcal{P}_{\Delta}(k), \quad (2)$$

where we have made use of a (gaussian) window function $W(k, R_H)$ to smooth out $\Delta(\vec{x})$ on the comoving horizon

length $R_H \sim 1/aH$ and $\mathcal{P}_{\Delta}(k) = (4k^2/9a^2H^2)^2\mathcal{P}_{\zeta}(k)$. The mass fraction β_M of the universe which ends up into PBHs at the time of formation is (for the non-Gaussian extension see Ref. [12])

$$\beta_M = \int_{\Delta_c}^{\infty} \frac{d\Delta}{\sqrt{2\pi}\sigma_{\Delta}} e^{-\Delta^2/2\sigma_{\Delta}^2} \simeq \frac{\sigma_{\Delta}}{\Delta_c\sqrt{2\pi}} e^{-\Delta_c^2/2\sigma_{\Delta}^2}. \quad (3)$$

It corresponds to a present fraction of dark matter $\rho_{\text{DM}}f_{\text{PBH}}(M) \equiv d\rho_{\text{PBH}}/d\ln M$ in form of PBHs of masses M

$$f_{\text{PBH}}(M) \simeq \left(\frac{\beta_M}{7 \cdot 10^{-9}}\right) \left(\frac{\gamma}{0.2}\right)^{1/2} \left(\frac{106.75}{g_*}\right)^{1/4} \left(\frac{M_{\odot}}{M}\right)^{1/2}. \quad (4)$$

Here $\gamma < 1$ accounts for the efficiency of the collapse and g_* is the number of effective relativistic degrees of freedom. We will assume $\gamma \simeq 0.2$ [13].

The key point is that, if there are large comoving curvature perturbations generated during the last stages of inflation, they inevitably act as a (second-order) source [14–17] of primordial GWs at horizon re-entry [18, 20]. By employing entropy conservation, we can relate the mass M of a PBH to the peak frequency of the GWs (not far from the peak frequency of the corresponding curvature perturbation) which collapses to form a PBH

$$M \simeq 50\gamma \left(\frac{10^{-9}\text{ Hz}}{f}\right)^2 M_{\odot}. \quad (5)$$

The expression (5) shows that the mass corresponding to the frequency where the Laser Interferometer Space Antenna (LISA) project [21] has the maximum sensitivity, $f_{\text{LISA}} \simeq 3.4$ mHz, is $M \simeq 10^{-12}M_{\odot}$.

The serendipity is that around this mass current observational constraints on the PBH abundances are basically

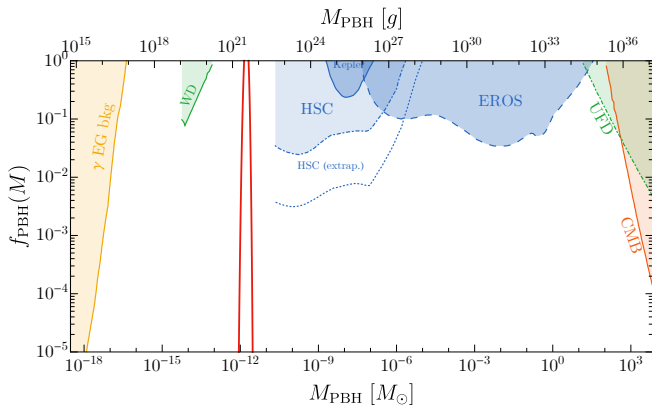


FIG. 1: The current experimental constraints on monochromatic spectra of PBH (from Ref. [23] and references therein): the observations of extra-galactic γ -ray background (yellow); the micro- and milli-lensing observations from Fermi, Eros, Kepler, Subaru HSC (blue); the dynamical constraints from White Dwarves and Ultra-Faint Dwarf galaxies (green); the constraints from the CMB (orange). The PBH abundance has been obtained for $A_s = 0.033$ and $k_* = 2\pi f_{\text{LISA}}$ in Eq. (6). For this choice, the integrated amount of PBHs corresponds to the totality of the dark matter of the universe.

absent [22], thus allowing $f_{\text{PBH}}(M) \simeq 1$, see Fig. 1. Indeed, the Subaru HSC microlensing measurements [24] must be cut around $10^{-11} M_\odot$ since below this mass the geometric optics approximation is no longer valid [22, 25]: the Einstein radius becomes smaller than the projected size of the star onto the lensing plane by a factor ten or so. As a consequence, the magnification is smaller than what required to detect a signal [22, 25]. Neutron star limits [26] are also not included as they depend on assumptions which are rather controversial on the dark matter density in globular clusters [22]. The curious reader can find a more expanded discussion in Appendix A of Ref. [27].

The optimal frequency range for the LISA observatory corresponds to the best shot for PBHs to account for all the dark matter. This is certainly an exciting coincidence.

In this letter we show that, if dark matter is composed of PBHs of masses around $10^{-12} M_\odot$, then LISA will measure the power spectrum of GWs inevitably associated to the production of the PBHs. Furthermore, and despite the fact that the primordial three-point correlator of the GWs is sizeable due to their intrinsically non-Gaussian nature (their small-scale source is second-order in the curvature perturbation, being the standard scale-invariant linear contribution subdominant), we show that LISA will not measure such large non-Gaussian signal. Indeed, the propagation effects from the point of production to the detector wipe out the initial correlation of the Fourier phases of the GWs, thus suppressing the GW three-point correlator. To the best of our knowledge, this point has not been made in the literature on similar subjects.

This short note contains only the main results; the reader can find the technical details in Ref. [27].

PBHs as dark matter. From the relation (5) we learn that PBHs of mass $\sim 10^{-12} M_\odot$ will form the totality of the dark matter if their corresponding mass fraction is $\beta_M \sim 6 \cdot 10^{-15}$. As a benchmark point, we take the comoving curvature perturbation power spectrum (augmented by the standard flat spectrum on large CMB scales) to be a peaked Dirac delta function

$$\mathcal{P}_\zeta(k) = A_s k_* \delta(k - k_*). \quad (6)$$

This shape has the huge advantage to let us perform all the calculations analytically. One finds the abundance in Fig. 1 for a representative choice of parameters. We have taken $k_* R_H \simeq 1$ and $\Delta_c \simeq 0.45$. The precise value of the threshold depends on the shape of the power spectrum [11], but this does not alter much the value of A_s , which is the most relevant quantity for the amount of GWs.

The power spectrum of GWs. The equation of motion for the GWs is obtained by expanding Einstein's equations up to second-order in perturbations

$$h''_{ij} + 2\mathcal{H}h'_{ij} - \nabla^2 h_{ij} = -4\mathcal{T}_{ij}{}^{\ell m} \mathcal{S}_{\ell m}, \quad (7)$$

where $'$ is the derivative with respect to the conformal time η , $\mathcal{H} = a'/a$ is the conformal Hubble parameter defined through the scale factor $a(\eta)$, and $\mathcal{S}_{\ell m}$ is the source term (in the radiation phase) [14]

$$\mathcal{S}_{ij} = 4\Psi \partial_i \partial_j \Psi + 2\partial_i \Psi \partial_j \Psi - \partial_i \left(\frac{\Psi'}{\mathcal{H}} + \Psi \right) \partial_j \left(\frac{\Psi'}{\mathcal{H}} + \Psi \right). \quad (8)$$

Notice that this source is second-order in the perturbations, which is the reason why the GWs generated at horizon re-entry, when PBHs are formed, are intrinsically non-Gaussian. Furthermore, the source is proportional to spatial derivatives of the perturbations and therefore one expects that the resulting bispectrum will be enhanced on equilateral configurations in momentum space. We come back to this point below. The projector $\mathcal{T}_{ij}{}^{\ell m}$ acting on the $\mathcal{S}_{\ell m}$ extracts its transverse and traceless part. We define it in Fourier space by using the chiral basis

$$\tilde{\mathcal{T}}_{ij}{}^{\ell m}(\vec{k}) = e_{ij}^L(\vec{k}) \otimes e^{L\ell m}(\vec{k}) + e_{ij}^R(\vec{k}) \otimes e^{R\ell m}(\vec{k}). \quad (9)$$

In Eq. (8) the scalar perturbation $\Psi(\eta, \vec{k})$ can be written in terms of the gauge-invariant comoving curvature perturbation as $(T(k\eta))$ being the transfer function during radiation) [28]

$$\Psi(\eta, \vec{k}) \equiv \frac{2}{3} T(k\eta) \zeta(\vec{k}), \quad (10)$$

where $T(x) = (9/x^2) [\sin(x/\sqrt{3})/(x/\sqrt{3}) - \cos(x/\sqrt{3})]$. A straightforward calculation leads to the current abundance of GWs [29]

$$\frac{\Omega_{\text{GW}}(f)}{\Omega_{r,0}} = \frac{c_g}{72} \int_{-\frac{1}{\sqrt{3}}}^{\frac{1}{\sqrt{3}}} dd \int_{\frac{1}{\sqrt{3}}}^{\infty} ds \left[\frac{(d^2 - 1/3)(s^2 - 1/3)}{s^2 - d^2} \right]^2$$

$$\cdot \mathcal{P}_\zeta\left(\frac{k\sqrt{3}}{2}(s+d)\right)\mathcal{P}_\zeta\left(\frac{k\sqrt{3}}{2}(s-d)\right)\mathcal{I}^2(d,s), \quad (11)$$

where $\Omega_{r,0}$ parametrises the current amount of radiation, $c_g \simeq 0.4$ accounts for the change of the number of relativistic degrees of freedom during the evolution, $\mathcal{I}^2 \equiv \mathcal{I}_c^2 + \mathcal{I}_s^2$, and

$$\begin{aligned} \mathcal{I}_c(x,y) = & 4 \int_1^\infty d\tau \tau (-\sin \tau) \left[2\mathcal{T}(x\tau)\mathcal{T}(y\tau) \right. \\ & \left. + \left(\mathcal{T}(x\tau) + x\tau \mathcal{T}'(x\tau) \right) \left(\mathcal{T}(y\tau) + y\tau \mathcal{T}'(y\tau) \right) \right], \end{aligned} \quad (12)$$

$\mathcal{I}_s(x,y)$ being the same function, but with $\sin \tau$ replaced by $(-\cos \tau)$. Their (long) analytical expressions can be found in Appendix D of Ref. [29] (see also Ref. [30]) and they take into account the effect of the radiation transfer function. For the power spectrum (6) we obtain (see also Refs. [18, 19])

$$\frac{\Omega_{\text{GW}}(f)}{\Omega_{r,0}} = \frac{A_s^2 c_g f^2}{15552 f_\star^2} \left(\frac{4f_\star^2}{f^2} - 1 \right) \theta \left(2 - \frac{f}{f_\star} \right) \mathcal{I}^2 \left(\frac{f_\star}{f}, \frac{f_\star}{f} \right), \quad (13)$$

where $f_\star = k_\star/2\pi$ and $\theta(x)$ is the step function. The current abundance of GWs is given in Fig. 2 with $k_\star \sim k_{\text{LISA}} = 2\pi f_{\text{LISA}}$ and $A_s \sim 0.033$. This shows that,

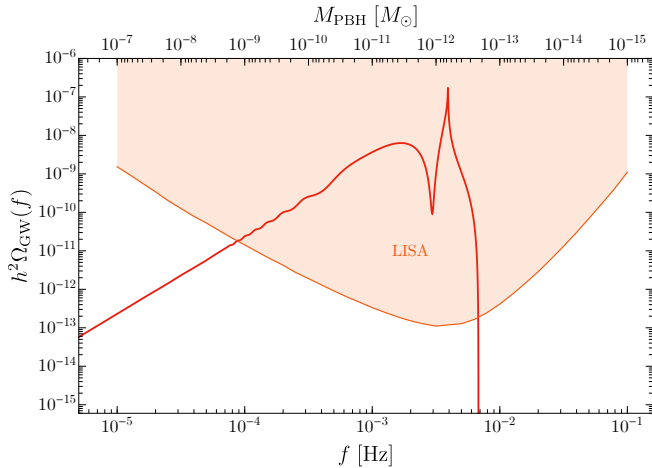


FIG. 2: The power spectrum of GWs generated by PBHs compared with the sensitivity for LISA estimated on the basis of the proposal [21]: the proposed design (4y, 2.5 Gm of length, 6 links) is anticipated to have a sensitivity in between those called C1 and C2 in Ref. [31]. The oscillatory behaviour and the spike is due to the trigonometric functions coming from the radiation transfer functions in \mathcal{I}^2 ; the spike is given by a resonant effect at $k \sim 2k_\star/\sqrt{3}$, as explained in Ref. [29].

if PBHs of masses $\sim 10^{-12} M_\odot$ form the dark matter (or even a fraction of it), LISA will measure the GWs popping out during the PBH formation time.

The primordial bispectrum of GWs. As we mentioned, being intrinsically non-Gaussian, the three-point correlator of the GWs is not vanishing. Its computation is straightforward and following the same steps of Ref. [29] one obtains

$$\begin{aligned} \langle h_{\lambda_1}(\eta, \vec{k}_1) h_{\lambda_2}(\eta, \vec{k}_2) h_{\lambda_3}(\eta, \vec{k}_3) \rangle' = & \left(\frac{8\pi}{9} \right)^3 \int d^3 p_1 \frac{1}{k_1^3 k_2^3 k_3^3 \eta^3} \\ & \cdot e_{\lambda_1}^*(\vec{k}_1, \vec{p}_1) e_{\lambda_2}^*(\vec{k}_2, \vec{p}_2) e_{\lambda_3}^*(\vec{k}_3, \vec{p}_3) \frac{\mathcal{P}_\zeta(p_1)}{p_1^3} \frac{\mathcal{P}_\zeta(p_2)}{p_2^3} \frac{\mathcal{P}_\zeta(p_3)}{p_3^3} \\ & \cdot \left[\cos(k_1 \eta) \mathcal{I}_c \left(\frac{p_1}{k_1}, \frac{p_2}{k_1} \right) + \sin(k_1 \eta) \mathcal{I}_s \left(\frac{p_1}{k_1}, \frac{p_2}{k_1} \right) \right] \\ & \cdot (1 \rightarrow 2 \text{ and } 2 \rightarrow 3) \cdot (1 \rightarrow 3 \text{ and } 2 \rightarrow 1), \end{aligned} \quad (14)$$

where $\vec{p}_2 = \vec{p}_1 - \vec{k}_1$, $\vec{p}_3 = \vec{p}_1 + \vec{k}_3$, and where $e_\lambda^*(\vec{k}, \vec{p}) = e_\lambda^{*ij}(\vec{k}, \vec{p}) p_i p_j$ are the polarisation tensors and $\lambda = \text{L, R}$. Our findings [27] (where we have calculated the bispectrum for other shapes of the curvature perturbation power spectrum) indicate that the bispectrum of GWs is dominated by the equilateral configuration, $k_1 \simeq k_2 \simeq k_3 \equiv k$. This is not unanticipated as they are sourced by gradients of the curvature perturbations when the latter re-enter the horizon. For the equilateral configuration and the Dirac delta shape (6) a lengthy, but straightforward calculation leads to the current bispectrum

$$\begin{aligned} \langle h_{\lambda_1}(\vec{k}_1) h_{\lambda_2}(\vec{k}_2) h_{\lambda_3}(\vec{k}_3) \rangle'_{\text{Eq}} = & \left(\frac{A_s a_{\text{eq}}}{k^2 k_\star \eta_{\text{eq}}} \right)^3 \frac{1024\pi^3}{729} \\ & \cdot \left| \frac{1}{\sqrt{2}} \mathcal{I} \left(\frac{k_\star}{k}, \frac{k_\star}{k} \right) \right|^3 \frac{\theta(\sqrt{3}k_\star - k)}{\sqrt{3k_\star^2/k^2 - 1}} \mathcal{D}_{\lambda_1 \lambda_2 \lambda_3} \left(\frac{k_\star}{k} \right), \end{aligned} \quad (15)$$

where $\mathcal{D}_{\lambda_1 \lambda_2 \lambda_3}(x) = 365/6912 - 61x^2/192 + 9x^4/16 - x^6/4$ for the RRR and LLL polarisations and $\mathcal{D}_{\lambda_1 \lambda_2 \lambda_3}(x) = x^6(-4 + 1/x^2)^2(-12 + 5/x^2)^2/768$ for the other combinations, see Fig. 3, and the subscript _{eq} stands for the equality epoch (we have taken $a_0 = 1$). Fig. 4 shows the contours of the (rescaled) bispectrum in the isosceles configurations. The generic case is reported in Ref. [27].

The importance of the propagation. Is the primordial bispectrum measurable by LISA? The answer seems to be unfortunately no. To the best of our knowledge this point has passed unnoticed in the recent literature on similar subject.

Non-Gaussianity is present whenever the Fourier phases of the observables out of which the bispectrum is constructed are correlated. This is the reason why non-Gaussianity is a synonym of “phase correlations”. On the contrary, the Fourier phases of a random Gaussian field have no correlation, they are randomly distributed [32]. The primordial bispectrum we have computed is non-vanishing precisely because inflation has introduced a synchronized clock among the different Hubble patches and the Fourier phases of the GWs are correlated when

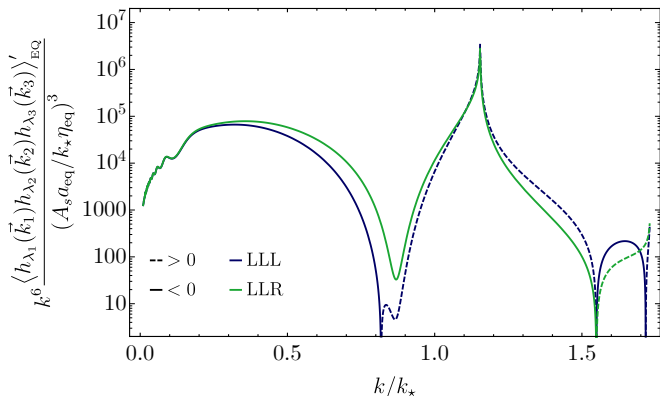


FIG. 3: The normalised shapes for the various primordial bispectra in the equilateral configurations.

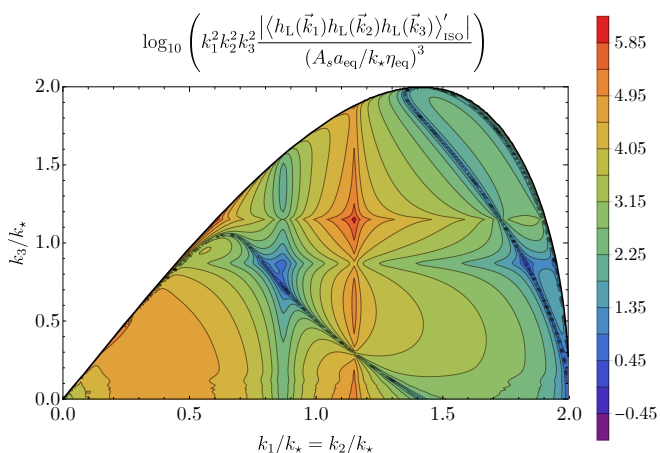


FIG. 4: Contour plot of the rescaled primordial bispectrum in the isosceles configurations.

generated. However, such a phase correlation is lost when the GWs propagate across the universe to get to the detector. To understand this point, one might think of the Shapiro time delay the GWs experience when propagating in an inhomogeneous universe. Since the time of arrival from different directions is much larger than the typical time scale involved in the problem, the GW phases are randomised. This suppresses the GW bispectrum at the detector.

To demonstrate this effect, let us consider the propagation of the GW during the matter-dominated phase. Furthermore, we work in the geometrical optic limit where the momentum of the propagating GW is much larger than the typical momentum associated to the gravitational potential, which we take to the linear order and in the long wavelength limit (hence the label L). The relevant equation is

$$h''(\vec{x}, \eta) + 2\mathcal{H}h'(\vec{x}, \eta) - \nabla^2 h(\vec{x}, \eta) = 4\Phi_L(\vec{x}, \eta)\nabla^2 h(\vec{x}, \eta). \quad (16)$$

In the limit in which $\Phi_L(\vec{x}, \eta)$ changes slowly with time

and with space, one can adopt a WKB approximation (alternatively one can separate fast and slow variables and Fourier transform only around the fast variable). In such a case one can check that the solution of the equation above can be written in momentum space as

$$h(\vec{k}, \eta) \propto \mathcal{I} e^{ik\eta} e^{2ik \int_{\eta_e}^{\eta} d\eta' \Phi_L(\hat{k}(\eta' - \eta_0), \eta')} + \mathcal{I}^* e^{-ik\eta} e^{-2ik \int_{\eta_e}^{\eta} d\eta' \Phi_L(-\hat{k}(\eta' - \eta_0), \eta')}, \quad (17)$$

where η_e is the emission time and we have located the detector at the origin of the spatial coordinates. The gravitational potential must be expanded along the line of sight

$$\Phi_L(\hat{k}(\eta' - \eta_0), \eta') = \int \frac{d^3 p}{(2\pi)^3} \Phi_L(\vec{p}, \eta') e^{i\vec{p} \cdot \hat{k}(\eta' - \eta_0)}. \quad (18)$$

We note that during the matter dominated era $\Phi_L(\vec{p}, \eta)$ is actually time independent. However $\Phi_L(\vec{x}, \eta)$ is evaluated along the path of the gravitational wave, and therefore it is time dependent. Here we have supposed that the GW is propagating along the direction \hat{k} . From the last expression one can already see that GWs arriving at the detector from various directions pick up different phases since along the different lines of sight they experience different values of the gravitational potential. Since Φ_L is not correlated with the short-scale ζ out of which the primordial GWs are built up, one can show that the bispectrum in the inhomogeneous universe, upon averaging over the many realisations of Φ_L , is largely suppressed with respect to the one in the homogeneous universe (15) (for more details, see Ref. [27])

$$\frac{\langle h_{\lambda_1}(\vec{k}_1) h_{\lambda_2}(\vec{k}_2) h_{\lambda_3}(\vec{k}_3) \rangle'_{\text{inh}}}{\langle h_{\lambda_1}(\vec{k}_1) h_{\lambda_2}(\vec{k}_2) h_{\lambda_3}(\vec{k}_3) \rangle'} \simeq e^{-0.8k^2 \eta_0^2 d_{\text{rms}}^2}, \quad (19)$$

where we have taken the equilateral limit, η_0 the current age of the universe, and $d_{\text{rms}} \sim 10^{-5}$ is the fractional rms Shapiro time delay [33]. This result can be thought as a consequence of the central limit theorem: the time delays would not affect the non-Gaussianity of the signal from a single line of sight, while averaging over the various directions suppresses the primordial three-point correlator. For other shapes, the suppression may be mitigated (for instance in the squeezed limit only the long mode momentum appears in the exponential), but it is still sizeable. This means unfortunately that propagation effects are harmful for any shape [27]. Nevertheless, they do not affect the power spectrum. It would be interesting to investigate the implications of the propagation effects beyond the geometrical optic limit, for example to the power spectrum. For instance, the scattering of the GWs off the gravitational potential background may change its polarisation. This certainly deserves more investigation.

Conclusions. If nature has chosen the option of making most (if not all) of the dark matter through PBHs,

it has definitely chosen the most economical one since no physics beyond the Standard Model is needed. In addition, if the PBHs forming the dark matter have a mass of the order of $10^{-12}M_{\odot}$ and they owe their origin to inflationary fluctuations, this option is not only still observationally viable, but testable. Indeed, we have shown that the unavoidable consequence of this scenario is the production of gravitational waves. We have proven that their signals will be tested by LISA both through the power spectrum and that, despite their intrinsically non-Gaussian nature, LISA should not measure any bispectrum. In fact, if no signatures of such gravitational relics is observed by LISA, we will readily conclude that the scenario described in this paper is not viable. On the contrary, even though new more robust constraints on f_{PBH} will appear, they will be satisfied decreasing A_s by a small amount (since f_{PBH} is exponentially sensitive to A_s), thus leaving anyway behind detectable GW signals. Of course, all these considerations leave open the possibility that the PBHs originate from mechanisms other than inflation.

Acknowledgments. We warmly thank the anonymous referee and A. Lewis for asking about the propagation effect, which has led to the revised version. We thank A. Katz for illuminating discussions on the microlensing and neutron star constraints on the PBH abundance. We thank C. R. Contaldi for discussions on the GW propagation. N.B. acknowledges partial financial support by the ASI/INAF Agreement I/072/09/0 for the Planck LFI Activity of Phase E2. He also acknowledges financial support by ASI Grant 2016-24-H.0. A.R. is supported by the Swiss National Science Foundation (SNSF), project *The Non-Gaussian Universe and Cosmological Symmetries*, project number: 200020-178787.

-
- [1] G. Bertone and T. M. P. Tait, *Nature* **562**, no. 7725, 51 (2018).
- [2] B. P. Abbott et al. [LIGO Scientific and Virgo Collaborations], *Phys. Rev. Lett.* **116**, 061102 (2016) [[gr-qc/1602.03837](#)].
- [3] S. Bird, I. Cholis, J. B. Muoz, Y. Ali-Hamoud, M. Kamionkowski, E. D. Kovetz, A. Raccanelli and A. G. Riess, *Phys. Rev. Lett.* **116**, no. 20, 201301 (2016) [[astro-ph.CO/1603.00464](#)].
- [4] J. García-Bellido, *J. Phys. Conf. Ser.* **840**, no. 1, 012032 (2017) [[astro-ph.CO/1702.08275](#)].
- [5] M. Sasaki, T. Suyama, T. Tanaka and S. Yokoyama, *Class. Quant. Grav.* **35**, no. 6, 063001 (2018) [[astro-ph.CO/1801.05235](#)].
- [6] L. Barack et al., [[gr-qc/1806.05195](#)].
- [7] P. Ivanov, P. Naselsky and I. Novikov, *Phys. Rev. D* **50**, 7173 (1994).
- [8] J. García-Bellido, A.D. Linde and D. Wands, *Phys. Rev. D* **54** (1996) 6040 [[astro-ph/9605094](#)].
- [9] P. Ivanov, *Phys. Rev. D* **57**, 7145 (1998) [[astro-ph/9708224](#)].
- [10] J. R. Espinosa, D. Racco and A. Riotto, *Phys. Rev. Lett.* **120** (2018) no.12, 121301 [[hep-ph/1710.11196](#)].
- [11] I. Musco, [[gr-qc/1809.02127](#)].
- [12] G. Franciolini, A. Kehagias, S. Matarrese and A. Riotto, *JCAP* **1803**, no. 03, 016 (2018) [[astro-ph.CO/1801.09415](#)].
- [13] B. J. Carr, *Astrophys. J.* **201** (1975) 1.
- [14] V. Acquaviva, N. Bartolo, S. Matarrese and A. Riotto, *Nucl. Phys. B* **667** (2003) 119 [[astro-ph/0209156](#)].
- [15] S. Mollerach, D. Harari and S. Matarrese, *Phys. Rev. D* **69** (2004) 063002 [[astro-ph/0310711](#)].
- [16] K. N. Ananda, C. Clarkson and D. Wands, *Phys. Rev. D* **75** (2007) 123518 [[gr-qc/0612013](#)].
- [17] D. Baumann, P. J. Steinhardt, K. Takahashi and K. Ichiki, *Phys. Rev. D* **76** (2007) 084019 [[hep-th/0703290](#)].
- [18] R. Saito and J. Yokoyama, *Prog. Theor. Phys.* **123**, 867 (2010) Erratum: [*Prog. Theor. Phys.* **126**, 351 (2011)] [[astro-ph.CO/0912.5317](#)].
- [19] E. Bugaev and P. Klimai, *Phys. Rev. D* **81**, 023517 (2010) [[astro-ph.CO/0908.0664](#)].
- [20] J. García-Bellido, M. Peloso and C. Unal, *JCAP* **1709**, no. 09, 013 (2017) [[astro-ph.CO/1707.02441](#)].
- [21] H. Audley et al., [[astro-ph.IM/1702.00786](#)].
- [22] A. Katz, J. Kopp, S. Sibiryakov and W. Xue, [[astro-ph.CO/1807.11495](#)].
- [23] K. Inomata, M. Kawasaki, K. Mukaida, Y. Tada and T. T. Yanagida, *Phys. Rev. D* **96** (2017) 043504 [[astro-ph.CO/1701.02544](#)].
- [24] H. Niikura et al., [[astro-ph.CO/1701.02151](#)].
- [25] K. Inomata, M. Kawasaki, K. Mukaida and T. T. Yanagida, *Phys. Rev. D* **97**, no. 4, 043514 (2018) [[astro-ph.CO/1711.06129](#)].
- [26] F. Capela, M. Pshirkov and P. Tinyakov, *Phys. Rev. D* **87**, no. 12, 123524 (2013) [[astro-ph.CO/1301.4984](#)].
- [27] N. Bartolo, V. De Luca, G. Franciolini, M. Peloso, D. Racco and A. Riotto, “Testing Primordial Black Holes as Dark Matter through LISA,” [[astro-ph.CO/1810.12224](#)], submitted to *Phys. Rev. D*.
- [28] D.H. Lyth and A. Riotto, *Phys. Rept.* **314** (1999) 1 [[hep-ph/9807278](#)].
- [29] J. R. Espinosa, D. Racco and A. Riotto, *JCAP* **1809**, no. 09, 012 (2018) [[hep-ph/1804.07732](#)].
- [30] K. Kohri and T. Terada, *Phys. Rev. D* **97** (2018) no.12, 123532 [[gr-qc/1804.08577](#)].
- [31] C. Caprini et al., *JCAP* **1604** (2016) no.04, 001 [[astro-ph.CO/1512.06239](#)].
- [32] T. Matsubara, *Astrophys. J. Suppl.* **170**, 1 (2007) [[astro-ph/0610536](#)].
- [33] W. Hu and A. Cooray, *Phys. Rev. D* **63**, 023504 (2001) [[astro-ph/0008001](#)].